Hidden XY structure of the bond-charge Hubbard model

Marco Roncaglia,[1] Cristian Degli Esposti Boschi,[2, *] and Arianna Montorsi[1]

[1]*Dipartimento di Fisica del Politecnico, corso Duca degli Abruzzi 24, I-10129 Torino, Italy*
[2]*CNR-IMM, Sezione di Bologna, via Gobetti 101, I-40129 Bologna, Italy*
(Dated: October 4, 2010)

The repulsive one-dimensional Hubbard model with bond-charge interaction (HBC) in the superconducting regime is mapped onto the spin-1/2 XY model with transverse field. We calculate correlations and phase boundaries, realizing an excellent agreement with numerical results. The critical line for the superconducting transition is shown to coincide with the analytical factorization line identifying the commensurate-incommensurate transition in the XY model.

The Hubbard Hamiltonian and its extensions are known to model several correlated quantum systems, ranging from high-T_c superconductors to cold fermionic atoms trapped into optical lattices [1]. In particular, the HBC model describes the interaction between fermions located on bonds and on lattice sites [2, 3]. This extension is considered to be especially relevant to the field of high-T_c superconductors [4]. In fact, it has recently been found [5, 6] that a superconducting phase takes place also for repulsive values of the on-site Coulomb interaction. The phase is characterized by incommensurate modulations in the charge structure factor. Its boundaries have been explored numerically, though their fundamental nature has not been understood yet.

We find that the explanation of the above features resides into the underlying effective model, which for the superconducting phase turns out to be the anisotropic XY chain in a transverse field. Such model is known to be equivalent to free spinless fermions and it is remarkable how it can faithfully describe quantities of a strongly correlated system like the HBC chain. Indeed, the mapping allows us to derive analytical expressions for both the critical line and correlations, reproducing with amazing accuracy the numerical data.

The model Hamiltonian for the HBC chain reads

$$\mathcal{H} = - \sum_{i\sigma} \left[1 - X \left(n_{i\bar\sigma} + n_{i+1\bar\sigma} \right) \right] \left(c_{i\sigma}^\dagger c_{i+1\sigma} + c_{i+1\sigma}^\dagger c_{i\sigma} \right)$$
$$+ U \sum_i n_{i\uparrow} n_{i\downarrow} - \frac{U}{2} \sum_{i\sigma} n_{i\sigma} \qquad (1)$$

where $\sigma = \uparrow, \downarrow$ ($\bar\sigma$ denoting the opposite of σ), and the operator $c_{i\sigma}^\dagger$ creates a fermion at site i with spin σ. Moreover $n_{i\sigma} = c_{i\sigma}^\dagger c_{i\sigma}$. The parameters U and X, expressed in units of the hopping amplitude, are the on-site and bond-charge Coulomb repulsion respectively.

While the HBC model cannot be exactly solved for all X, there are two integrable point at $X = 0$ and $X = 1$, for all values of U. The former is the well-known Hubbard model which is solvable by Bethe Ansatz. The integrability of the case $X = 1$ is due to the fact that the empty

and the doubly occupied sites in this case are indistinguishable, and the same holds for the $\uparrow$ and $\downarrow$ spins in the singly occupied sites, so that the model can be rephrased in terms of tight-binding spinless fermions in 1D [7]. In addition, the number of double occupancies turns out to be a conserved quantity.

In the general case, Eq.(1) can be fruitfully recast passing to a slave boson representation. One can make the transformation $|0\rangle \rightarrow e_i |0\rangle$, $c_{i\sigma}^\dagger |0\rangle \rightarrow f_{i\sigma}^\dagger |0\rangle$ and $c_{i\uparrow}^\dagger c_{i\downarrow}^\dagger |0\rangle \rightarrow d_i |0\rangle$, where empty and doubly occupies sites are bosons, while the single occupations are fermions. The hard-core constraint $e_i^\dagger e_i + d_i^\dagger d_i + \sum_\sigma f_{i\sigma}^\dagger f_{i\sigma} = 1$ completes the identification. Then, the c-fermions are $c_{i\sigma}^\dagger = f_{i\sigma}^\dagger e_i + d_i^\dagger f_{i\bar\sigma}$ and $n_{i\sigma} = c_{i\sigma}^\dagger c_{i\sigma} = f_{i\sigma}^\dagger f_{i\sigma} + d_i^\dagger d_i$. The total number of particles is $N = N_f + 2N_d$. The filling factor is $\nu = N/L$, with $0 \leq \nu \leq 2$. Accordingly, we have $\nu_e + \nu_f + \nu_d = 1$ and $\nu = \nu_f + 2\nu_d$. After the substitution, the Hamiltonian becomes $\mathcal{H} = \sum_{i\sigma} \mathcal{H}_{i\sigma}$, where

$$\mathcal{H}_{i\sigma} = -\frac{U}{2} f_{i\sigma}^\dagger f_{i\sigma} + \left[f_{i\sigma}^\dagger f_{i+1,\sigma} \left(t_X d_{i+1}^\dagger d_i - e_{i+1}^\dagger e_i \right) \right.$$
$$\left. - s_X f_{i\sigma}^\dagger f_{i+1,\bar\sigma}^\dagger \left(e_{i+1} d_i + d_{i+1} e_i \right) + \text{H.c.} \right], \qquad (2)$$

with $t_X = 1 - 2X$, and $s_X = 1 - X$. It can be recognized that the first two terms describe the kinetic energy of a single electron (hole) with spin σ in a background of empty (doubly occupied) sites, whereas the third term describes the transformation of two opposite spins into an empty and a doubly occupied site. Since the coefficient s_X turns out to give the smallest contribution for $X > 2/3$, it is not surprising that the exact solution obtained assuming $s_X = 0$ (and arbitrary t_X) [8] shares in this regime many features of the ground state of the true model, obtained by numerical investigation [9]. To some extent, these features hold within the range $X > X_c = 1/2$, where X_c is the value at which t_X changes sign. This is true in particular as for the presence of phase coexistence of domains formed by only empty or doubly occupied sites, in which the single particles move. On the other hand, fixing $s_X = 0$ yields to a critical curve $U_{PS} = 4X$ for the stability of the phase separated region, whereas the superconducting transition takes place

(only for $s_X \neq 0$) at a value U_{SC} which is well below that line. Since the role of empty and doubly occupied sites, as well as the conservation of their number, appears to be the same as for $s_X = 0$ [10] also in the superconducting case, one can infer that it is just the motion of the single electrons and holes which determines the change $U_{PS} \to U_{SC}$ for $s_X \neq 0$. In this paper, we assume this point of view: *treating the empty and doubly occupied states as the vacuum in which the single particles move.*

Let us go back to Eq.(2) and consider what happens at $s_X \neq 0$. The $SU(2)$ charge symmetry is broken down to $U(1)$, which merely describes the conservation of the number of fermions. The large spin degeneracy is removed and it is like as if the fermionic dynamics is influenced by the background imposed by the bosons and viceversa. This picture is correct as far as the spin and charge degrees of freedom are not separated. For $X \lesssim 1$, the pair creation term in Eq.(2) induces short-ranged antiferromagnetic (AFM) correlations in both spin and pseudospin degrees of freedom. Since at half-filling the probabilities of having an empty and a doubly occupied sites are identical and coincide with $1/2$, we can approximate the term $\langle e^{\dagger}_{i+1} e_i - t_X d^{\dagger}_{i+1} d_i \rangle \approx X$. Thus, in this case the kinetic energy term in $\mathcal{H}_{i\sigma}$ becomes $-X f^{\dagger}_{i\sigma} f_{i+1\sigma} + (X-1) f^{\dagger}_{i\sigma} f^{\dagger}_{i+1,\bar{\sigma}} + \text{H.c.}$ where the term $f^{\dagger}_{i\sigma} f^{\dagger}_{i+1,\bar{\sigma}}$ always takes place due to the bosonic AFM correlations. Both the bosonic species are considered as a unique vacuum for the fermions f.

Assuming the existence of AFM correlations also in the fermionic variables, we can drop the spin indices. The effect of $f^{\dagger}_i f^{\dagger}_{i+1}$ is to open a gap at the Fermi level, hence reducing considerably the ground state (GS) energy. This mechanism is analogous to what happens in the case of the Peierls instability (in that case the gap is opened by the dimerization) where the bosons here play the role of the phonons that distort the lattice. So, we obtain a free-spinless fermion model $\mathcal{H}^{(f)} = \sum_{i=1}^{L} \mathcal{H}_i^{(f)}$, where

$$\mathcal{H}_i^{(f)} = -X \left(f^{\dagger}_i f_{i+1} + \frac{1-X}{X} f^{\dagger}_i f^{\dagger}_{i+1} + \text{H.c.} \right) - \frac{U}{2} f^{\dagger}_i f_i . \tag{3}$$

It is instructive to notice that even in this form one can recover the exact solution of the case $X = 1$. Indeed a straghtforward diagonalization in Fourier space gives $H = -2 \sum_k [\cos k + U/4] f^{\dagger}_k f_k$. The fermions fill the negative energy states up to the Fermi point $k_f = \pi \nu_f$. The saturation occurs for $U_c = -4 \cos(\pi\nu)$ for $0 < \nu < 2$.

In the general case, $\mathcal{H}^{(f)}$ can be easily shown to be equivalent to the following XY model in a transverse field

$$\mathcal{H}_{XY} = E_0 - \frac{1}{\zeta} \sum_{i=1}^{L} \left[\frac{1+\gamma}{2} \sigma^x_i \sigma^x_{i+1} + \frac{1-\gamma}{2} \sigma^y_i \sigma^y_{i+1} + h \sigma^z_i \right] \tag{4}$$

where $\gamma = \frac{1-X}{X}$, $h = \frac{U}{4X}$, $E_0 = -\frac{UL}{4}$ and $\zeta = \frac{1}{X}$, at half filling. As usual we have applied the Jordan-Wigner

transformation $\sigma^z_i = 2 f^{\dagger}_i f_i - \mathbb{I}$, $\sigma^+_i = f^{\dagger}_i K_{i-1}$, $\sigma^-_i = K^{\dagger}_{i-1} f_i$ with $K_l = \prod_{k=1}^{l} (-\sigma^z_k) = \exp[i\pi \sum_{k=1}^{l} n_k]$.

AFM correlations in both bosonic and fermionic particles are here assumed on the intuitive basic observation of the reduction of GS energy by means of the pair creation terms. A more rigorous approach would involve a self-consistent determination of the hopping coefficients in the quadratic model in which the spin labels are retained. Such approach allows to extend the analysis away from half filling and in magnetic field, and goes beyond the purpose of the present paper. We dedicate a forthcoming extended manuscript to a self-consistent approach.

In what follows, we examine some important consequences that can be derived from the exact solution of the XY model, written in Eq.(4).

As known, the Hamiltonian (4) can be diagonalized: $H = E_0 + \frac{1}{\zeta} \sum_{k \in BZ} \Lambda_k \left(\beta^{\dagger}_k \beta_k - \frac{1}{2} \right)$, where the sum is performed in the Brillouin zone (BZ), and the dispersion relations are $\Lambda_k = 2\sqrt{(\cos k + h)^2 + \gamma^2 \sin^2 k}$. Given the positiveness of Λ_k, the GS energy E_{GS} is determined by the vacuum of the Bogoliubov quasiparticles β_k, giving $E_{GS} = E_0 - \frac{1}{2L} \sum_{k \in BZ} \Lambda_k$. By taking the thermodynamic limit $L \to \infty$, we get an energy density $e_{GS} = -\frac{U}{4} - \frac{X}{4\pi} \int_{-\pi}^{\pi} dk \Lambda_k$.

We have compared the outcomes of our mapping with numerical calculations using the density matrix renormalization group (DMRG) [12]. In particular, we used extrapolations in $1/L$ of data collected by selecting 7 finite-system sweeps and 1024-1152 states. Numerical and analytical results of the energy density at $X = 0.8$ are displayed in table I.

U	e_{GS}^{num}	e_{GS}^{th}	ν_d^{num}	ν_d^{th}	q/π	ψ/π
0	-0.5390	-0.54612	0.2511	$1/4$	14/30	$1/2$
0.5	-0.670	-0.67708	0.216	0.22611	14/30	0.44841
1	-0.81544	-0.82011	0.19016	0.20164	12/30	0.39539
1.5	-0.9717	-0.97565	0.173	0.17588	10/30	0.33914
2.5	-1.3300	-1.3287	0.1063	0.11488	6/30	0.20116

Table I: Comparison between various quantities defined in the text computed either numerically (num) with DMRG or analytically by means of the equivalent XY model (th) for $X = 0.8$, both for periodic boundary conditions. The latter is treated directly in the thermodynamic limit, while the former are extrapolated to $L \to \infty$ from finite-size data. The characteristic wavenumber q is extracted from Fourier transforms at $L = 30$.

An important feature of the XY chain is the presence of a factorization line $h^2 + \gamma^2 = 1$, which corresponds to a commensurate-incommensurate (CIC) transition. In the HBC model this transition is mapped analytically into

$$U_{SC} = 4\sqrt{2X - 1}. \tag{5}$$

Such transition was discovered numerically in Ref.[5] and separates a incommensurate singlet superconducting
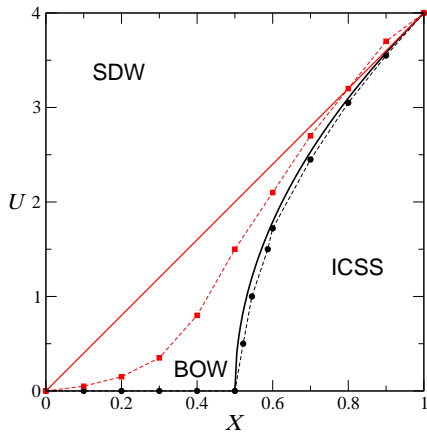
Figure 1: Comparison between the phase diagram of the HBC chain, calculated numerically in Ref.[6] (symbols with dashed lines) and the phase diagram obtained from the mapping onto the XY model in transverse field (continuous lines). The upper curves correspond to the spin gap transition where spin excitations become gapless, while the lower curves mark the transition into the ICSS phase where the charge compressibility diverges.

(ICSS) phase from a bond ordered wave (BOW) phase [6]. As seen in Fig.1, the curve obtained with our mapping describes rather accurately the numerical data of the transition.

Along the factorization line the GS in the $S = 1/2$ model is written as $\otimes_{i=1}^{L}|\phi\rangle$, where $|\phi\rangle = \cos\frac{\theta}{2}|\uparrow\rangle + \sin\frac{\theta}{2}|\downarrow\rangle$, with $\cos\theta = [(1-\gamma)/(1+\gamma)]^{1/2} = \alpha$. Here the local magnetization is $2\nu_f - 1 = \alpha = \sqrt{2X-1}$. Accordingly, the number of double occupations along the factorization line at half filling is $\nu_d = (1-\alpha)/4 = (1-\sqrt{2X-1})/4$. In the rest of the phase diagram, the transverse magnetization of the XY chain is given by $\langle\sigma_i^z\rangle = \frac{2}{L}\sum_{k\in BZ}(h+\cos k)\Lambda_k^{-1}$. The diverging charge compressibility of the ICSS phase is explainable simply by observing that adding two particles produce the conversion of an empty site onto a doubly occopied one, without changing the energy in the XY representation.

In addition, the XY model in 1D is known to undergo a quantum phase transition along line $h = 1$, belonging to the universality class of the classical Ising model in 2D. This translates directly into the line $U = 4X$ in the phase diagram of the HBC model (see Fig.1). The latter coincides with the critical line of stability of PS (U_{PS}) in the integrable case $s_X = 0$, and is close to the numerical critical line between the spin density wave (SDW) and the BOW phase in Fig. 1, at least for X close to 1. Moreover, the line $\gamma = 1$, which is known to describe the Ising model in a transverse field, here corresponds to the case $X = 1/2$. While it is questionable whether the assumptions that have originated our approximations for the ICSS phase are still valid in the above limiting cases, one can recognize that instead at the very crucial critical
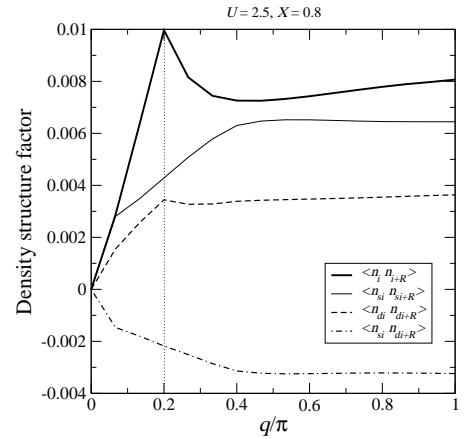

Figure 2: Analysis of the various contributions [see Eq.(7)] to the static structure factor (Fourier transform) of the density correlation function for the HBC model ($L = 30$) with the parameters reported in the legend. The vertical line corresponds to ψ/π (see table I).

point $X = 1/2$ and $U = 0$, our system described in Eq.(1) is mapped into nothing but the Ising model.

From the seminal paper of Barouch and McCoy on the statistical mechanics of the XY model [11], it is known that the oscillation wavenumber of the correlator $\rho_{xx}(R) = \langle\sigma_i^x\sigma_{i+R}^x\rangle$ in the incommensurate region $h^2 + \gamma^2 < 1$ is

$$\tan\psi = \frac{\sqrt{1-\gamma^2-h^2}}{h} = \sqrt{\frac{2X-1}{(U/4)^2}-1}, \qquad (6)$$

with a period $R_0 = 2\pi/\psi$.

A first striking observation is the fact that the correlations of the *total* density exhibit a peak very close to the characteristic wavenumber ψ in Eq.(6): in the last two columns of table I we report the wavevector q at which the total density structure factor has a peak (see an example in fig. 2). For $X = 0.9$ and $U = 3$ with $L = 32$ the peak is located at $q/\pi = 0.1875$ while $\psi/\pi = 0.18342$.

The appearance of the peak at wavenumber Q in the Fourier transform of a correlation function that decays as $\cos(QR)\exp(-R/\xi)/R^a$ is related also to the exponent a: the smaller is a the sharper is the peak. In particular for $a = 2$ which is the case for the correlation $\rho_{zz}(R) = \langle\sigma_i^z\sigma_{i+R}^z\rangle$ of the XY model, the peak it not visibile at all, despite the fact that the oscillations actually *have* characteristic wavenumber 2ψ. Hence, it is worth to inspect in more detail the origin of the peaks observed numerically. Since the local density operator n_i in terms of single and double occupancies n_{si} and n_{di} is given by $n_i = n_{si} + 2n_{di}$, the correlation function of the total density decomposes in the following parts

$$\langle n_i n_{i+R}\rangle = \langle n_{si} n_{si+R}\rangle + 4\langle n_{di} n_{di+R}\rangle$$
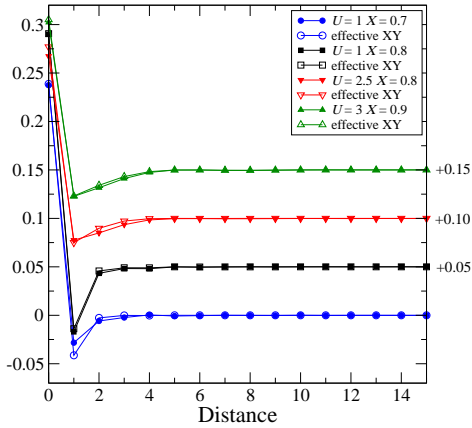$$+ 2\langle n_{di} n_{si+R}\rangle + 2\langle n_{si} n_{di+R}\rangle. \qquad (7)$$

Figure 3: Comparison of the connected real-space correlation functions $N_s(R)$ (at half-filling) and $\rho(R)$ for the HBC and XY model, respectively (see text for definitions based on singly occupied sites operators). The parameters of the two models are related by mapping as $\gamma = (1 - X)/X$ and $h = U/4X$. All the DMRG calculations for the HBC model and the analytical experessions of the curves for the XY model refer to $L = 50$. From top to bottom the data have been offset by $+0.15$, $+0.10$ and $+0.05$ for the sake of clarity.

It turns out that the peak in the static structure factor is not due to the first term, but it is instead provided by $\langle n_{di}n_{di+R} \rangle$, as shown in Fig.2 for the test case $X = 0.8$ and $U = 2.5$, although we obtained the same qualitative picture at $U = 1$.

According to our mapping, we can compare directly the connected correlator $N_s(R) = \langle n_{si}n_{si+R} \rangle - \langle n_{si} \rangle^2$ in the HBC model with the density correlation function $\rho(R) = \langle f_i^\dagger f_i f_{i+R}^\dagger f_{i+R} \rangle - \langle f_i^\dagger f_i \rangle^2$ for the spinless fermions with Hamiltonian (3). The calculation of the latter is omitted here since it is quite lengthy, though it simply involves a standard application the Wick theorem. The fully fermionic correlator $N_s(R)$ and the spinless fermions correlator $\rho(R)$ are compared in Fig.3 for various choices of the parameters U and X in the ICSS phase of our starting system (i.e. the incommensurate one in the XY model); the agreement in real space is generally very good. Such behaviour of $N_s(R)$ is not obvious a priori in the HBC model and we interpret it as a remarkable nontrivial prediction of our mapping.

In summary, we have studied the Hubbard model with bond-charge interaction in the superconducting regime, unveiling its underlying XY structure. We have shown that at half filling the numerical critical line for superconductivity coincides with remarkable accuracy to the analytical factorization curve that marks the CIC transition of the anisotropc XY model in a transverse field. Exploting the mapping for the calculation of correlations in the effective model has allowed us to predict rather accurately the peak in the charge structure factor of the original model. The results confirm a posteriori the crucial role of short range AF correlations and spin degrees of freedom as to the onset of superconductivity. The ultimate presence of the latter is however to be ascribed to the interplay of the spin with the charge degrees of freedom, the superconducting properties being absent from the incommensurate phase of the free fermions model.

Based on the success of the present mapping, a number of further result are now in order. First, since the one-dimensionality of the model is not crucial to the mapping, the latter should hold in higher dimension as well. In 2D, the numerical investigation of the XY model has been largely explored in the literature: this could provide useful hints on the type of phase diagram which characterizes the 2D HBC model. Moreover, it would be interesting to understand the implications on the HBC model of a non-vanishing string order parameter which is peculiar of the XY model in transverse field. Finally, we expect that a similar mapping should hold also in the strongly repulsive regime $U \to \infty$, since in that case no doubly occupied sites occur, and it is still quite natural to assume short range AFM order of single particles.

* On leave from CNISM, Unità di Ricerca del Dip. di Fisica dell'Università di Bologna, where this work was started.

[1] I. Bloch, J. Dalibard and W. Zwerger, Rev. Mod. Phys. **80**, 885 (2008).

[2] J. T. Gammel and D. K. Campbell, Phys. Rev. B **60**, 71 (1988).

[3] For reviews see G. I. Japaridze and A. P. Kampf, Phys. Rev. B **59**, 12822 (1999); M. Nakamura, T. Okano and K. Itoh, Phys. Rev. B **72** 115121 (2005); A. Aligia, and A. Dobry, preprint, arXiv:1009.4113, and references therein; as well as reference [6] below.

[4] J. E. Hirsch, Physica C **158** 326 (1989); J. E. Hirsch and F. Marsiglio, Phys. Rev. B **39**, 11515 (1989).

[5] A. Anfossi, C. Degli Esposti Boschi, A. Montorsi, and F. Ortolani, Phys. Rev. B **73** , 085113 (2006).

[6] A.A. Aligia *et al.*, Phys. Rev. Lett. **99**, 206401 (2007).

[7] L. Arrachea and A. A. Aligia, Phys. Rev. Lett. **73**, 2240 (1994).

[8] A. Montorsi, J. Stat. Mech. L09001 (2008)

[9] A. Anfossi, C. Degli Esposti Boschi and A. Montorsi, Phys. Rev. B **79**, 235117 (2009)

[10] A. Anfossi, L. Barbiero, and A. Montorsi, Phys. Rev. A **80**, 043602 (2009)

[11] E. Barouch and B. M. McCoy, Phys. Rev. A **3**, 786 (1971).

[12] U. Schollwöck, Rev. Mod. Phys. **77**, 259 (2005).